Published in final edited form as:
Cancer Res. 2015 April 1; 75(7): 1255–1264. doi:10.1158/0008-5472.CAN-14-1801.

Adaptive upregulation of EGFR limits attenuation of tumor growth by neutralizing IL-6 antibodies with implications for combined therapy in ovarian cancer

C. Milagre[1], **G. Gopinathan**[1], **G. Everitt**[1], **R.G. Thompson**[1], **H. Kulbe**[1], **H. Zhong**[2], **R.E. Hollingsworth**[2], **R. Grose**[1], **D. Bowtell**[3], **D. Hochauser**[4], and **F.R. Balkwill**[1]

[1]Barts Cancer Institute, Queen Mary University of London, Charterhouse Square, London EC1M 6BQ UK

[2]MedImmune, One MedImmune Way, Gaithersburg, MD 20878 USA

[3]Cancer Genomics and Genetics Program, Peter MacCallum Cancer Centre, Research Division, Peter MacCallum Cancer Centre, Locked Bag 1 A'Beckett St, Melbourne 8006, VIC. Australia

[4]UCL Cancer Institute, University College London, 72 Huntley St, London WC1E 6BT UK

Abstract

Excess production of the pro-inflammatory interleukin IL-6 has both local and systemic tumor-promoting activity in many cancers, including ovarian cancer. However, treatment of advanced ovarian cancer patients with a neutralizing IL-6 antibody yielded little efficacy in a previous Phase II clinical trial. Here we report results that may explain this outcome, based on the finding that neutralizing antibodies to IL-6 and STAT3 inhibition are sufficient to up-regulate the EGFR pathway in high-grade serous and other ovarian cancer cells. Cell treatment with the EGFR inhibitor gefitinib abolished upregulation of the EGFR pathway. Combining neutralizing IL-6 antibodies and gefitinib inhibited malignant cell growth in 2D and 3D culture. We found that ErbB-1 was localized predominantly in the nucleus of ovarian cancer cells examined, contrasting with plasma membrane localization in lung cancer cells. Treatment with anti-IL-6, gefitinib or their combination all led to partial restoration of ErbB-1 on the plasma membrane. *In vivo* experiments confirmed the effects of IL-6 inhibition on the EGFR pathway and the enhanced activity of a combination of anti-IL-6 antibodies and gefitinib on malignant cell growth. Taken together, our results offer a preclinical rationale to combine anti-IL-6 and gefitinib to treat patients with advanced stage ovarian cancer.

Introduction

Abnormal regulation of interleukin-6 (IL-6) and its major downstream transcription factor STAT3 is a feature of many human cancers (1). Constitutive production of IL-6 and STAT3 occurs downstream of some oncogenic mutations in malignant cells and there is strong evidence that IL-6 is tumor-promoting in many different experimental cancer models (2).

IL-6 is implicated in the pathophysiology of high-grade serous ovarian cancer, HGSC and clear cell ovarian cancer, CCC (3-5). We previously demonstrated that constitutive IL-6 production by malignant cells is a major regulator of cancer-related inflammation and

Europe PMC Funders Author Manuscripts

cytokine networks in HGSC, having important local and systemic tumor-promoting actions (3, 4, 6).

In mouse models, anti-IL-6 antibodies have anti-tumor activity, inhibiting communication between malignant cells and stroma, reducing the leukocyte infiltrate and angiogenesis, with evidence of vessel normalization (3). We reported some activity in a Phase II clinical trial of an anti-IL-6 antibody in patients with advanced HGSC, but sustained responses were not achieved (3). One of the seventeen HGSC patients treated had a partial response to anti-IL-6 therapy, seven others had periods of disease stabilization, and systemic levels of some cytokines, inflammatory and tumor biomarkers were reduced during the therapy but rose as the patients regressed.

There could be many reasons for the low efficacy of IL-6 blockade in patients with HGSC. Our previous research would suggest that a major factor might be the complexity of malignant cell cytokine production. As we have shown that inflammatory cytokines such as IL-6 interact in networks with other inflammatory mediators and growth factors in ovarian cancer cells (4, 7, 8), we hypothesized that inhibiting constitutive IL-6 production by malignant cells may induce reciprocal feedback regulation in other signaling pathways that compensates for their action and reduces efficacy of neutralizing anti-IL-6 antibodies.

To investigate this hypothesis, we treated ovarian cancer cells with neutralizing anti-IL-6 antibodies and studied changes in intracellular signaling pathways. We found that inhibiting IL-6 signaling in these cells and ovarian cancer xenografts up-regulated EGFR signaling and ERK activation. A combination of EGFR inhibition by gefitinib and neutralizing anti-IL-6 antibodies had enhanced anti-cancer activity.

Materials and Methods

Ovarian cancer cell lines

The IGROV-1 line was recently characterized as a hypermutated line but does have TP53 and BRCA2 mutations typical of HGSC (9). The AOCS1 cell line was established from a patient diagnosed with HGSC, Silverberg grade 3, with <1cm residual disease after primary surgery. The patient had 18 months progression-free survival after 6 cycles carboplatin & paclitaxel adjuvant chemotherapy but showed no response to Line 2 liposomal doxorubicin. The cell line AOCS1 was established from material taken at second relapse. AOCS1 stains with antibodies to EPCAM and Pax8. The G33 cell line was established in our laboratory from omental metastases of a patient with HGSC after chemotherapy. It has a p53 mutation W146* and is positive for EPCAM and Pax8. Quality control of all cell lines was carried out by frequent STR analysis (Eurofins MWG, Ebersberg), mycoplasma testing (InvivoGen, USA) and cell lines were used for 4-5 passages before new cells were recovered from frozen master stocks. Cells were cultured RPMI 1640 supplemented with 10% FCS and 1% pen-strep. Cells were counted using a Vi-cell cell counter (Beckman Coulter) on days 3 and 7. All technical and experimental replicates were repeated in triplicate.

Primary cancer cells

All the tissue samples were obtained under the guidelines of the Human Tissue Authority Act 2004, and all patients had given prior consent under the Research Ethical Committee Project reference 10/H0304/14.

Treatments

Cells were treated with 10μg/ml anti-IL-6 antibody (MEDI5117) (Medimmune, Gaithersburg, MD), and 1μM Gefitinib (AstraZeneca AZD1839). MEDI5117 is a human immunoglobulin G1 kappa (IgG1κ) monoclonal antibody that binds to IL-6 with sub-pM affinity and neutralizes it by preventing the binding to interleukin 6 receptor (IL-6R). MEDI5117 was generated using phage display technology. It bears a triple mutation (referred to as YTE) in the Fc domain of the heavy chain that extends its stability in circulation. MEDI5117 is active in several preclinical cancer models, including NSCLC, prostate cancer, breast cancer, and ovarian cancer xenografts in mice (Manuscript in preparation, Medimmune). An IgG1 isotype control antibody was generated by MedImmune and was used at the same concentration as anti-IL-6 antibody (10μg/ml).

Protein extraction from mouse tumors

75mg of tumor tissue was lysed with 1ml of ice-cold lysis buffer (150mM NaCl 20mM Tris, pH 7.5 1mM EDTA(1mM EGTA(1% Triton X-100) with protease and Phosphatase Inhibitors. Samples were then dissociated using gentleMACS Dissociator. After dissociation, samples were centrifuged at 1500 rpm for 2 minutes. Samples are always kept on ice between procedures. Next, using a probe sonicator set at 40% amplitude, tissues were sonicated for 5-15 seconds bursts. Sonicated samples were then rotated for 30 minutes at 4°C followed by a centrifugation for 15 minutes at 13,200 rpm at 4C. The pellet was discarded and protein concentration measured. Lysates were frozen at −80°C until loaded on gels.

Western Blotting

Cells were washed with PBS and harvested using RIPA Buffer (R0278, Sigma UK) with 1× proteinase inhibitors. Protein quantification was performed using the Bradford reagent (Sigma-Aldrich), according to the manufacturer's instructions. Cell extracts (25 μg) were run on a NuPAGE® Novex® 4-12% Bis-Tris Gel, 1.5 mm and transferred to a nylon membrane. The membrane was blocked overnight (4°C in PBS with 0.1% Tween and 5% milk powder) and probed using the following antibodies: Phospho-Stat3 (Tyr705) (1:1000 #9145, Cell Signaling), Stat3 (1:1000 #4904, Cell Signaling), p-ERK (1:1000 sc-7383, Santa Cruz), ERK (1:1000 #9102, Cell Signaling), phospho-ErbB-1 (1:1000 #2220, Cell Signaling), ErbB-1 (1:1000 2232, Cell Signaling), phospho-ErbB-4 (1:500 #3790, Cell Signaling), ERbB-4 (1:1000 #4795, Cell Signaling), TNFα (1:1000 ab6671, Abcam), Jagged1 (1:1000 SC-8303, Santa Cruz), α-tubulin (1:2000 sc-8035, Santa Cruz), Lamin A/C (1:2000 #2032, Cell Signaling), β-Actin (1:5000 A5316, Sigma). A rabbit or mouse horseradish peroxidase-conjugated secondary antibody (GE Healthcare, Chalfont St Giles, UK) incubation allowed visualization using enhanced chemiluminescence (ECL) (GE Healthcare). Protein concentration equivalence was confirmed by anti–β-actin antibody.

Quantifying western blots

Western blots were quantified using ImageJ analysis. The images were set to grayscale 8-type bit and a rectangular box was drawn to enclose a single lane. The box was then selected as the first lane and the same process was repeated for the remaining of the lanes. The relative density of the contents of each lane was then plotted as histograms and a straight line was drawn underneath where the peak ends to subtract any background. The wand tool was then used to get the measurements of each profile. The ratios were obtained by normalizing the density of each band to its total protein or loading control (10).

Immunoprecipitation

2×10^7 cells were homogenized in 1 ml of RIPA buffer (R0278, Sigma) containing phosphate inhibitor cocktail (P-5726, Sigma) and incubated on ice for 10minutes. Samples were centrifuged at 10,000 g for 10 min at 4°C, and supernatant was then transferred to a new tube. Protein concentration of the supernatant was determined. Lysates were cleaned using Rabbit IgG control and 20µl of Protein A/G PLUS-Agarose beads (sc-2003, SantaCruz) for 30min at 4°C. Beads were pelleted by centrifugation at 2,500rpm for 5min and lysates transferred to a clean tube. Samples were immunoprecipitated for 2 hours at 4°C using 500µg of total lysate and 2µg of appropriate antibody (ErbB-1 or STAT3). Lysates were then rotated overnight at 4°C with 20µl of A/G PLUS Agarose beads. The next day, the Agarose beads were washed four times in RIPA buffer followed by a 5min centrifugation at 1,000×g at 4°C. After final wash, supernatant was discarded and pellet was resuspended in 40µl of 1× electrophoresis buffer, boiled for 5 min at 70°C before separation using SDS-PAGE.

Immunofluorescence staining and nuclear quantification

1×10^4 cells were plated on coverslips (Nalge Nunc International, ThermoFisher Scientific, Rochester, NY, US) and kept in culture with RPMI 1640 medium supplemented with 10%FCS and 1% pen-strep. Next day, medium was replaced with serum-free medium. Cells were treated with 10µg/ml of anti-IL-6 antibody and/or 1µM Gefitinib and incubated at 37°C, 5% CO_2 for 24 hours. Supernatants were discarded and cells were fixed with 4% paraformaldehyde for 30 min, permeabilized in 0.5% Triton X-100 for 30min and washed 3 times in 0.1% Triton X-100. Staining was performed overnight with ErbB-1 (1:50 Alexa Fluor 488, Santa Cruz) or isotype control (1:200, R&D systems). Primary antibody was washed with PBS. Slides were counterstained with DAPI Prolong Gold (Invitrogen) and images captured by Nikon Eclipse 80i microscope and Image-Pro Plus software (Media Cybernetics).

Nuclear and cytoplasmic quantification of ErbB-1 immunofluorescent data was done using MetaMorph Microscopy Automation & Image Analysis Software following the instructions provided by the manufacturer.

siRNA transfection

2×10^4 cells were plated in a 6 well plate and transfected with 100pmol of siRNA pool of 4 different targeting sequences or non-specific Scramble control (stock concentration at 50pmol/µl) in 250µl serum-free medium. 4µl of lipofectamine 2000 (Life technologies UK) was also added to the mix. Samples were vortexed and incubated at room temperature for 15

minutes. After 6-8 hours, medium was removed and replaced with fresh RPMI 1640 supplemented with 10% FCS. 24 hours later, protein quantification was accessed and 20μg of cell lysate was analyzed by western blot.

Immunohistochemistry

Paraffin-embedded sections of tumors collected from mouse xenograft were stained with antibodies for Phospho-p44/42 MAPK (Erk1/2) (Thr202/Tyr204)(cell signaling, 9106S), Tyr705 phospho-STAT3 (Cell Signaling, 9145) and Y1068 Phospho-EGFR (Cell Signaling, 8543S). Slides were counterstained with haematoxylin. Negative controls were isotype matched. The conditions used for staining with individual antibodies were in accord with manufacturers' recommendations.

Growth of tumors in mice and bioluminescence imaging

A total of 10×10^6 luciferase-expressing IGROV-1 cells (IGROV-1luc) were injected intraperitoneally (i.p.) into 20g 6 to 8 week-old female BALB/c nu/nu mice (purchased from Charles River, UK Ltd). These cell lines were generated as previously published (11). Mice were observed daily for tumor growth and killed once they reached end points as defined in our Home Office Project Licence PPL 70/7411 (20% increase in abdominal distension). All observable peritoneal tumors were dissected and weighed at the end of the experiment. There were 8 mice in each group and two separate experiments were conducted.

Statistical analysis

Statistical analyses were carried out using Prism Graph Pad software. Statistical significance was calculated using ANOVA and Student's t test. Findings are presented as standard error of the mean (SEM).

Results

IL-6 inhibition activates EGFR signaling in ovarian cancer cells

We initially tested the effect of neutralizing antibodies to IL-6 on newly established high grade serous ovarian cancer cell lines (AOCS1, G33), on freshly isolated cells from HGSC ascites and on IGROV-1, a previously characterized IL-6 producing ovarian cancer line of uncertain histotype but with TP53 and BRCA2 mutations (9). We first asked if treating cells with a neutralizing antibody to IL-6 had an impact on other intracellular signaling pathways that were likely to be active in these cells, with a focus on ErbB signaling. Cells were cultured for 3 and 7 days in the presence of an anti-IL-6 antibody (MEDI5117) or an IgG isotype control (Figure 1A, for AOCS1 and primary cells, Supplementary Figure 1 A for IGROV-1 cells).

Western blot analysis and quantification showed, as expected, that inhibition of IL-6 reduced STAT3 phosphorylation (Supplementary Figure 1A-C,). However, in the presence of IL-6 inhibition, the cells activated alternative signaling pathways through ErbB-1, ErbB-4 and ERK phosphorylation (Figure 1A, Supplementary Figure 1). The results in Figure 1 and Supplementary Figure 1 were consistent in repeated experiments. To demonstrate this we show mean results of the key finding from three experiments with the AOCS1 cell line (See

Supplementary Figure 2). We also observed that IL-6 inhibition leads to a modest increase in release of EGFR ligands (HB-EGF, TGFα and EGF) by the cells (data not shown).

EGFR family members are over-expressed in approximately 70% of ovarian cancers and this is associated with a poor prognosis (12) (13). However, single agent targeting of ErbB-1 has shown minimal activity in ovarian cancer patients (13, 14). Our results suggested that combination therapies targeting both EGFR and IL-6 pathways might have therapeutic potential. To investigate this, cells were treated with gefitinib, a selective inhibitor of the EGFR tyrosine kinase by binding to the ATP-binding site of the enzyme (15). Gefitinib treatment alone decreased phosphorylation of ErbB-1 and ERK but induced pSTAT3 activation (Figure 1B), as previously described (16). In AOCS1, a combination of gefitinib and the anti-IL-6 antibody also decreased ErbB-1 phosphorylation and pERK levels, but in this instance pSTAT3 activation decreased as well (Figure 1B). Similar results were obtained with the G33 cell line (Figure 1B, right panel) and IGROV-1 cells (data not shown). Quantification of these blots can be found in Supplementary Figure 3.

Combined therapy that targets IL-6 and EGFR pathways reduces proliferation in 2D and 3D cultures

To investigate the biological relevance of these observations we studied growth of the cell lines in the presence of anti-IL-6 and gefitinib. AOCS1 and IGROV-1 cells were treated with the anti-IL-6 antibody, gefitinib or their combination. In 2D culture (Figure 2A, B), IL-6 inhibition had no effect on cell proliferation as we have previously reported (3). Gefitinib significantly reduced cell counts and this growth inhibition was greater in the combination treatment group (Figure 2A,B). We next used a 3D cell culture system adapted from (17) that mimics the microenvironment of the human omentum, a major site of peritoneal cancer metastasis. The model consisted of fibroblasts embedded in a collagen matrix covered by a layer of primary human mesothelial cells. AOCS1 cells were grown for two weeks in this system and then the area of malignant cell growth was measured using ImageJ (Figure 2C,D). Both anti-IL-6 and gefitinib reduced malignant cell growth in the organotypic cultures and the greatest inhibition was seen in the combination treatment group (Figure 2D).

ErbB-1 has a nuclear localization in ovarian cancer cells and this is altered by IL-6 inhibition

We also investigated the effects of anti-IL-6 on EGFR in the cells using immunofluorescence and confocal microscopy. Confocal images and z-stack analysis of the images revealed that ErbB-1 was primarily located in the nucleus (nErbB-1) in all three lines (Figure 3A-C and Supplementary Figure 4A, z-stack top panel). This observation has been previously reported in some ovarian cancer cell lines and human ovarian cancer biopsies (18). Upon treatment with anti-IL-6 antibody for 24 hours, nErbB-1 staining was reduced and in some of the cells analyzed, relocalized to the plasma membrane (Figure 3A-C and Supplementary Figure 4A, z-stack bottom panel). As an experimental control we also studied A549 cells, a lung adenocarcinoma cell line with well-characterized cell surface expression of ErbB1. ErbB-1 remained at the plasma membrane whether or not the cells were treated with anti-IL-6 (Figure 3D). In a control for the specificity of antibody staining,

IGROV-1 cells were treated with siRNA to ErbB-1 or a scramble control, resulting in an almost complete removed staining in both nucleus and cytoplasm (Figure 3E,F). We then carried out nuclear and cytoplasmic fractionation of cells treated either with IgG control antibody or the anti-IL-6 antibody. Anti-IL-6 treatment resulted in a reduction of ErbB-1 in the nuclear fraction of IGROV-1 cells at 24 hours and three days treatment with anti-IL-6 (Fig 3G,H, Supplementary Figure 4B). Similar results were obtained with AOCS1 (Supplementary Figure 5A). Tubulin and nuclear lamin antibodies were used to test separation of cytoplasmic and nuclear fraction respectively, confirming the purity of the fractions (Figure 3G,H and Supplementary Figure 5A).

Anti-IL-6 antibodies and β-importin silencing both disrupt ErbB-1 nuclear localization

Next, we tested the effects of gefitinib plus/minus anti-IL-6 on nErbB-1 (Figure 4A). Gefitinib, anti-IL-6 treatment and their combination relocalized ERB-1 expression to the membrane.

The presence of growth factor receptors in the nucleus is well documented in several human cancers and nuclear translocation of EGFR family members has been extensively described (19-21), but the mechanism of translocation and the role of EGF receptor family members in the nucleus of malignant cells is still unclear (22-24). Others have reported that ErbB-1 co-localizes and interacts with β-importin in thyroid cells in order to be translocated into the nucleus (19, 22, 24). We therefore treated AOCS1 cells with β-importin siRNA. Knock down of β-importin reduced nErbB-1; this was not observed when AOCS1 cells were treated with ‘scrambled’ control siRNA (Figure 4A).

Data from the above experiments were quantified using metamorph analysis software and correspond to an average of five microscope fields per condition (Figure 4B). The intensity of nErbB-1 was reduced after treating the cells with either anti-IL-6 antibody, gefitinib or the combination of both agents (Figure 4B). Studies have suggested that ErbB-1 interacts with other transcription factors, such as STAT3, in the nucleus (25). Thus, we next performed co-immunoprecipitation to see if ErbB1 co-localized with STAT3. Figure 4C shows that immunoprecipitation of ErbB-1 pulls down STAT3 in AOCS1 cells, thus suggesting that IL-6 inhibition and consequent STAT3 reduction in the nucleus might offer a possible explanation for the reduction of ErbB-1 in the nucleus.

Our work so far has shown that ovarian cancer cells are able to compensate for reduced autocrine IL-6 signaling by up regulating the EGFR signaling pathway. In addition, it appears that in HGSC cell lines, ErbB1 is located to the nucleus and that treatment with either anti-IL-6 antibody or gefitinib, or their combination, lead to reinstatement of ErbB1 on the plasma membrane of AOCS1, G33 and IGROV-1 cells.

To test if treatment of ovarian cancer cells with both gefitinib and anti-IL-6 antibodies was able to enhance anti-tumor activity, we conducted experiments in peritoneal xenografts.

Gefitinib in combination with anti-IL-6 reduces tumor weight in mouse xenografts

We grew IGROV-1 cells as intraperitoneal xenografts in nude mice and treated the mice with the anti-human IL-6 antibody, gefitinib or both in combination. Results of two independent experiments were combined and data are shown in Figure 5.

Twenty-one days after treatment tumors were extracted and weighed. IL-6 inhibition reduced tumor weight as previously shown (3) (Figure 5A). Gefitinib treatment alone was able to significantly reduce tumor weight compared with the IgG control group. However, the combination of anti-IL-6 antibodies and gefitinib was the most effective in reducing tumor weight (Figure 5A).

Histological analysis of tumors collected from mice revealed a reduction of pSTAT3 with IL-6 inhibition, which was accompanied by an increase in pERK and pErbB-1 (Figure 5B). We next analyzed the cellular localization of ErbB-1 in the xenograft sections. Results show that tumors from control mice have nuclear ErbB-1. Tumors from mice treated with anti-IL-6, gefitinib or the combination have mainly plasma membrane ErbB-1 (Figure 5C) as previously suggested in Figure 3. To assess further the effect of anti-IL-6 on EGFR and IL-6 pathways *in vivo*, we extracted protein from the mouse tumors and assessed the expression of pSTAT3, pErbB-1 and pERK. IL-6 inhibition *in vivo* effectively reduced pSTAT3 activation and led to an increase in pErbB-1 and pERK (Figure 5D). In addition, we used these lysates to demonstrate that *in vivo*, IL-6 inhibition reduces TNFα and Jagged1 levels (Figure 5E), two components of the IL-6 tumor cytokine network that we previously described (3).

A summary diagram of our results is shown in Figure 6.

Discussion

While many pre-clinical studies and clinical observations suggest that IL-6 inhibitors would be of therapeutic benefit in patients with advanced cancers (1, 3, 6, 8), clinical trials have not shown conclusive evidence of activity, apart from in patients with Castleman's disease which is primarily driven by IL-6. In our clinical trial of a therapeutic anti-IL-6 antibody in patients with high-grade serous ovarian cancer, we found some evidence of disease stabilization but this was not sustained (3). All our evidence to date would suggest that the effects of IL-6 in this disease are driven by constitutive malignant cell production of IL-6 (3, 6-8). Thus we investigated the possibility that IL-6 inhibition might induce some reciprocal feedback regulation of other pathways.

In our study, treatment with the anti-IL-6 antibody did not completely abrogate STAT3 phosphorylation. IL-6 is not the only cytokine/growth factor that activates STAT3 hence neutralizing IL-6 would not always be expected to completely abrogate STAT3 phosphorylation. However, experimental data in the literature would suggest that partial STAT3 abrogation is therapeutically significant. For example, tumor cells that become dependent on persistent STAT3 signaling are more sensitive to STAT3 inhibition than normal cells (26). In experiments with a lymphoma model, partial downregulation of STAT3 (40%) was responsible for strong antitumor effects *in vivo* (27) and in colon cancer

xenografts partial inhibition of JAK/STAT3 signalling pathway is enough to suppress the growth of colon cancer xenografts(28).

In addition, our previous research on cytokine networks in malignant cells (7) would suggest that rational combination of therapies targeting the malignant cells and their interaction with the microenvironment are worthy of investigation. Links between the IL-6 and EGFR pathway have already been reported (29-32). For instance, EGFR stimulation of ovarian cancer cell lines increased IL-6 production (29), but none of the cell lines used in the latter paper are now thought to be of HGSC origin (9). In addition, in human lung adenocarcinomas, mutations in the EGFR kinase domain stimulated STAT3 activation via IL-6 production (30).

Hence we decided to study the influence of IL-6 inhibition on EGFR signaling. The cell lines that we used in our experiments did not have EGFR mutations (data not shown). In this paper we have used cell lines and primary tumor cells from peritoneal cancers that are collectively termed ‘ovarian’ cancers. As explained in the methods section, AOCS1 and G33 are new cell lines recently established from HGSC patient biopsies. The primary cancer cells used in our experiments were from pathologically confirmed HGSC patient ascites. The cancer of origin of the ovarian cancer cell line IGROV-1 is uncertain (33). We have included it in our experiments as an example of an IL-6 producing cell line that forms peritoneal xenografts in nude mice (3).

Our results led us to test combinations of anti-IL-6 and gefitinib and our experiments suggested that this may have therapeutic potential. However, our recent increased understanding of the natural history and genetic drivers of HGSC (34-36) means that some of the cell lines and syngeneic models (e.g.ID8 cells) are not relevant models of the disease. A new genetic model of HGSC has recently been published (37) and in the next few years as this, or transplantable cell lines derived from such mice, become more widely used, we should have more appropriate models of HGSC for preclinical experiments. IL-6 produced by malignant cells has paracrine actions not only on angiogenesis but also on the extent and phenotype of the leukocyte infiltrate (3, 7). Hence a combination of IL-6 and EGFR inhibition may be more powerful in a syngeneic model or in patients with HGSC compared to the results described here using immunocompromised mouse xenograft models.

Nuclear EGFR signaling is thought to confer resistance to various anti-cancer therapies (23) and may explain the poor response of ovarian cancer patients to gefitinib (38). All the cells used in this paper were resistant to the anti-EGFR antibody cetuximab (data not shown) and there was no interaction between cetuximab and anti-IL-6. The nuclear expression of ErbB-1 may explain this finding (20). The partial restoration of membrane-localized ErbB-1 by anti-IL-6 antibody treatment may not be sufficient to permit inhibition by cetuximab.

As both gefitinib and therapeutic anti-IL-6 antibodies have been given safely to patients with ovarian cancer, and both targets are implicated in this disease, specifically HGSC, we suggest that our data provide a rationale for testing their combination.

Supplementary Material

Refer to Web version on PubMed Central for supplementary material.

Acknowledgments

D Hochhauser acknowledges support from Cancer Research UK Programme Grant C2259/A16569

F Balkwill acknowledges support from Cancer Research UK Programme Grant C587/A16354

D Bowtell acknowledges support from the Australian National Health and Medical Research Council Grant APP1044447.

References

1. Koji Taniguchia MK. IL-6 and related cytokines as the critical lynchpins between inflammation and cancer. Seminars in Immunology. 2014; 26:54–74. [PubMed: 24552665]
2. He G, Dhar D, Nakagawa H, Font-Burgada J, Ogata H, Jiang Y, et al. Identification of liver cancer progenitors whose malignant progression depends on autocrine IL-6 signaling. Cell. 2013; 155:384–96. [PubMed: 24120137]
3. Coward JKH, Chakravarty P, Leader D, Vassileva V, Leinster DA, Thompson R, Schioppa T, Nemeth J, Vermeulen J, Singh N, Avril N, Cummings J, Rexhepaj E, Jirström K, Gallagher WM, Brennan DJ, McNeish IA, Balkwill FR. Interleukin-6 as a therapeutic target in human ovarian cancer. Clinical Cancer Research. 2011; 15:6083–96. [PubMed: 21795409]
4. Kulbe H, Chakravarty P, Leinster DA, Charles KA, Kwong J, Thompson RG, et al. A dynamic inflammatory cytokine network in the human ovarian cancer microenvironment. Cancer Res. 2012; 72:66–75. [PubMed: 22065722]
5. Anglesio MS, George J, Kulbe H, Friedlander M, Rischin D, Lemech C, et al. IL6-STAT3-HIF signaling and therapeutic response to the angiogenesis inhibitor sunitinib in ovarian clear cell cancer. Clin Cancer Res. 2011; 17:2538–48. [PubMed: 21343371]
6. Stone RL, Nick AM, McNeish IA, Balkwill F, Han HD, Bottsford-Miller J, et al. Paraneoplastic thrombocytosis in ovarian cancer. N Engl J Med. 2012; 366:610–8. [PubMed: 22335738]
7. Kulbe H, Thompson R, Wilson JL, Robinson S, Hagemann T, Fatah R, et al. The inflammatory cytokine tumor necrosis factor-alpha generates an autocrine tumor-promoting network in epithelial ovarian cancer cells. Cancer Res. 2007; 67:585–92. [PubMed: 17234767]
8. Kulbe H, Hagemann T, Szlosarek PW, Balkwill FR, Wilson JL. The inflammatory cytokine tumor necrosis factor-alpha regulates chemokine receptor expression on ovarian cancer cells. Cancer Res. 2005; 65:10355–62. [PubMed: 16288025]
9. Domcke S, Sinha R, Levine DA, Sander C, Schultz N. Evaluating cell lines as tumour models by comparison of genomic profiles. Nat Commun. 2013; 4:2126. [PubMed: 23839242]
10. Gassmann M, Grenacher B, Rohde B, Vogel J. Quantifying Western blots: pitfalls of densitometry. Electrophoresis. 2009; 30:1845–55. [PubMed: 19517440]
11. Benard J, Da Silva J, De Blois MC, Boyer P, Duvillard P, Chiric E, et al. Characterization of a human ovarian adenocarcinoma line, IGROV1, in tissue culture and in nude mice. Cancer Res. 1985; 45:4970–9. [PubMed: 3861241]
12. Kandala PK, Wright SE, Srivastava SK. Blocking epidermal growth factor receptor activation by 3,3′-diindolylmethane suppresses ovarian tumor growth in vitro and in vivo. J Pharmacol Exp Ther. 2012; 341:24–32. [PubMed: 22205686]
13. Colomiere M, Findlay J, Ackland L, Ahmed N. Epidermal growth factor-induced ovarian carcinoma cell migration is associated with JAK2/STAT3 signals and changes in the abundance and localization of alpha6beta1 integrin. Int J Biochem Cell Biol. 2009; 41:1034–45. [PubMed: 18930836]
14. Sheng Q, Liu J. The therapeutic potential of targeting the EGFR family in epithelial ovarian cancer. Br J Cancer. 2011; 104:1241–5. [PubMed: 21364581]

15. Erjala K, Sundvall M, Junttila TT, Zhang N, Savisalo M, Mali P, et al. Signaling via ErbB2 and ErbB3 associates with resistance and epidermal growth factor receptor (EGFR) amplification with sensitivity to EGFR inhibitor gefitinib in head and neck squamous cell carcinoma cells. Clin Cancer Res. 2006; 12:4103–11. [PubMed: 16818711]
16. Wu K, Chang Q, Lu Y, Qiu P, Chen B, Thakur C, et al. Gefitinib resistance resulted from STAT3-mediated Akt activation in lung cancer cells. Oncotarget. 2013
17. Kenny HAKT, Yamada SD, Lengyel E. Use of a novel 3D culture model to elucidate the role of mesothelial cells, fibroblasts and extra-cellular matrices on adhesion and invasion of ovarian cancer cells to the omentum. Int J Cancer. 2007; 1:1463–72. [PubMed: 17546601]
18. Xia W, Wei Y, Du Y, Liu J, Chang B, Yu YL, et al. Nuclear expression of epidermal growth factor receptor is a novel prognostic value in patients with ovarian cancer. Mol Carcinog. 2009; 48:610–7. [PubMed: 19058255]
19. Wang YN, Lee HH, Lee HJ, Du Y, Yamaguchi H, Hung MC. Membrane-bound trafficking regulates nuclear transport of integral epidermal growth factor receptor (EGFR) and ErbB-2. J Biol Chem. 2012; 287:16869–79. [PubMed: 22451678]
20. Li C, Iida M, Dunn EF, Ghia AJ, Wheeler DL. Nuclear EGFR contributes to acquired resistance to cetuximab. Oncogene. 2009; 28:3801–13. [PubMed: 19684613]
21. Lo HW, Ali-Seyed M, Wu Y, Bartholomeusz G, Hsu SC, Hung MC. Nuclear-cytoplasmic transport of EGFR involves receptor endocytosis, importin beta1 and CRM1. J Cell Biochem. 2006; 98:1570–83. [PubMed: 16552725]
22. Lo HW, Hung MC. Nuclear EGFR signalling network in cancers: linking EGFR pathway to cell cycle progression, nitric oxide pathway and patient survival. Br J Cancer. 2006; 94:184–8. [PubMed: 16434982]
23. Wei-Chien Huanga Y-JC, Mien-Chie Hunga. Implication of nuclear EGFR in the development of resistance to anticancer therapies. BioMedicine. 2011; 1:2–10.
24. Brand TM, Iida M, Li C, Wheeler DL. The nuclear epidermal growth factor receptor signaling network and its role in cancer. Discov Med. 2011; 12:419–32. [PubMed: 22127113]
25. Lo HW, Hung MC. Nuclear EGFR signalling network in cancers: linking EGFR pathway to cell cycle progression, nitric oxide pathway and patient survival. Br J Cancer. 2007; 96(Suppl):R16–20. [PubMed: 17393580]
26. Yu H, Jove R. The STATs of cancer--new molecular targets come of age. Nat Rev Cancer. 2004; 4:97–105. [PubMed: 14964307]
27. Scuto A, Kujawski M, Kowolik C, Krymskaya L, Wang L, Weiss LM, et al. STAT3 inhibition is a therapeutic strategy for ABC-like diffuse large B-cell lymphoma. Cancer Res. 2011; 71:3182–8. [PubMed: 21521803]
28. Phesse TJ, Buchert M, Stuart E, Flanagan DJ, Faux M, Afshar-Sterle S, et al. Partial inhibition of gp130-Jak-Stat3 signaling prevents Wnt-beta-catenin-mediated intestinal tumor growth and regeneration. Sci Signal. 2014; 7:ra92. [PubMed: 25270258]
29. Alberti C, Pinciroli P, Valeri B, Ferri R, Ditto A, Umezawa K, et al. Ligand-dependent EGFR activation induces the co-expression of IL-6 and PAI-1 via the NFkB pathway in advanced-stage epithelial ovarian cancer. Oncogene. 2012; 31:4139–49. [PubMed: 22158046]
30. Gao SP, Mark KG, Leslie K, Pao W, Motoi N, Gerald WL, et al. Mutations in the EGFR kinase domain mediate STAT3 activation via IL-6 production in human lung adenocarcinomas. J Clin Invest. 2007; 117:3846–56. [PubMed: 18060032]
31. Aaronson DS, Muller M, Neves SR, Chung WC, Jayaram G, Iyengar R, et al. An androgen-IL-6-Stat3 autocrine loop re-routes EGF signal in prostate cancer cells. Mol Cell Endocrinol. 2007; 270:50–6. [PubMed: 17374439]
32. Wang Y, van Boxel-Dezaire AH, Cheon H, Yang J, Stark GR. STAT3 activation in response to IL-6 is prolonged by the binding of IL-6 receptor to EGF receptor. Proc Natl Acad Sci U S A. 2013; 110:16975–80. [PubMed: 24082147]
33. Silvia, Domcke; Rileen, Sinha; Levine, Douglas A.; Chris, Sander; Nikolaus, Schultz. Evaluating cell lines as tumour models by comparison of genomic profiles. Nature Communications. 2013

34. Bashashati A, Ha G, Tone A, Ding J, Prentice LM, Roth A, et al. Distinct evolutionary trajectories of primary high-grade serous ovarian cancers revealed through spatial mutational profiling. J Pathol. 2013; 231:21–34. [PubMed: 23780408]

35. Vaughan S, Coward JI, Bast RC Jr. Berchuck A, Berek JS, Brenton JD, et al. Rethinking ovarian cancer: recommendations for improving outcomes. Nat Rev Cancer. 2011; 11:719–25. [PubMed: 21941283]

36. Berns EM, Bowtell DD. The changing view of high-grade serous ovarian cancer. Cancer Res. 2012; 72:2701–4. [PubMed: 22593197]

37. Perets R, Wyant GA, Muto KW, Bijron JG, Poole BB, Chin KT, et al. Transformation of the fallopian tube secretory epithelium leads to high-grade serous ovarian cancer in Brca;Tp53;Pten models. Cancer Cell. 2013; 24:751–65. [PubMed: 24332043]

38. Murphy M, Stordal B. Erlotinib or gefitinib for the treatment of relapsed platinum pretreated non-small cell lung cancer and ovarian cancer: a systematic review. Drug Resist Updat. 2011; 14:177–90. [PubMed: 21435938]

Europe PMC Funders Author Manuscripts

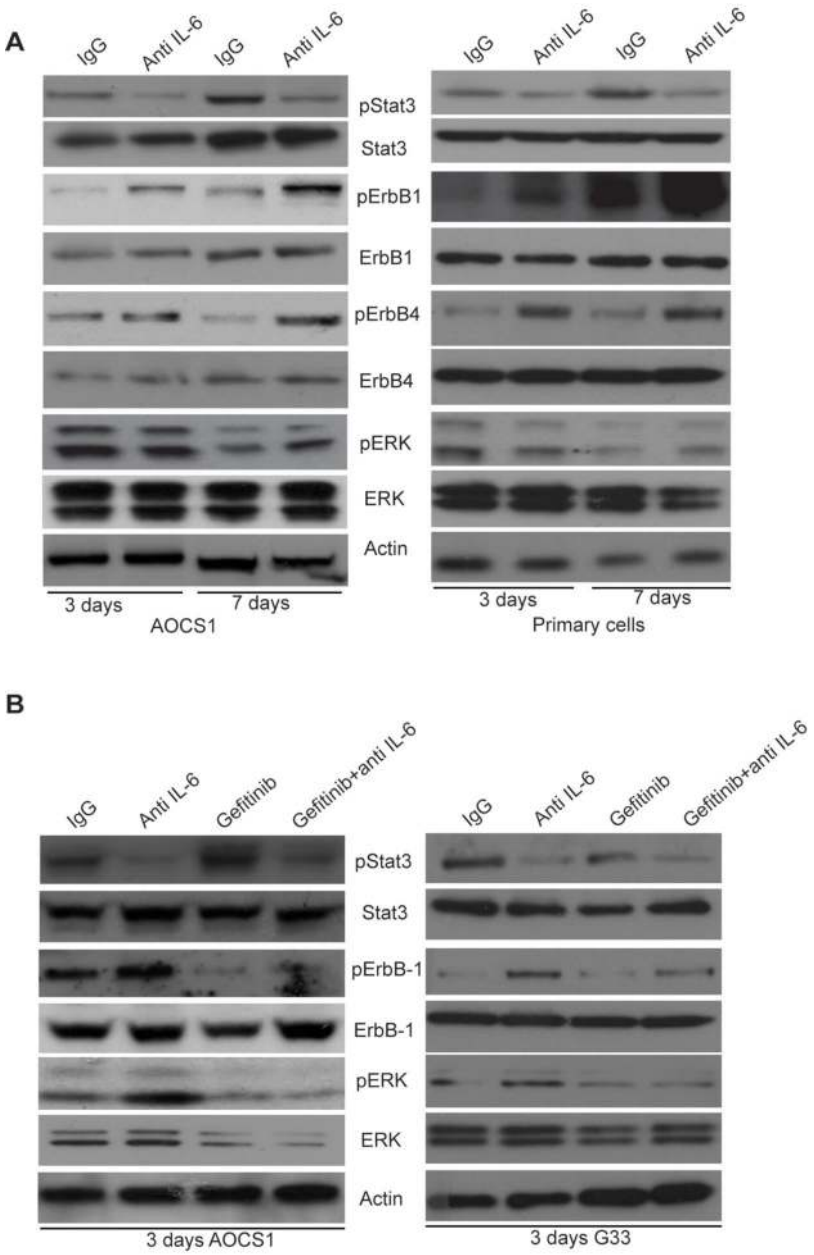

Figure 1. IL-6 inhibition activates the EGFR signaling pathway

A. 2×10^5 HGSC cells (AOCS1) and primary cells were treated with anti-IL-6 antibody (10μg/ml) for 3 days and 7 days and lysates were analyzed by Western blotting. Data shown are typical of 3 independent experiments. **B.** 2×10^5 AOCS1 and G33 HGSC cells were treated with anti-IL-6 antibody (10μg/ml), gefitinib (1μM) alone or with a combination of both inhibitors.

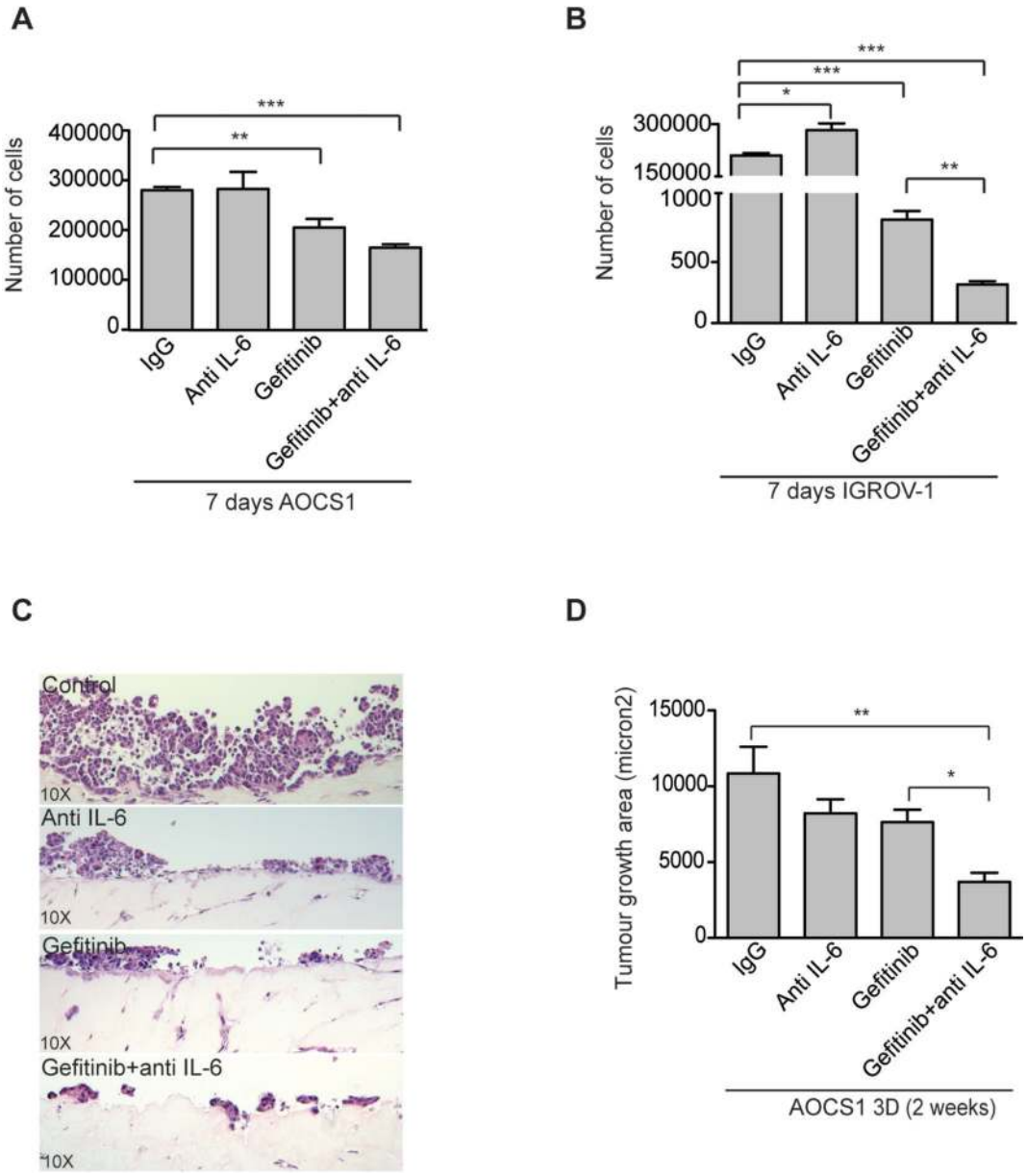

Figure 2. Anti-IL-6 combined with gefitinib reduces proliferation *in vitro* and tumor growth area on 3D culture models

A, B. AOCS1 and IGROV-1 cells were treated with an anti-IL-6 antibody (10μg/ml) and/or gefitinib (1μM) for 7 days. **C,D.** H&E staining sections of 3D cultures of AOCS1 cells. AOCS1 cells were seeded into on top of a layer of mesothelial cells and fibroblasts embedded in collagen. Data in A, B and D are shown as mean ± SEM of 3 independent experiments. Statistic analysis was performed and is shown as (*) p ≤0.05: (**) p ≤0.01; (***) p ≤0.001.

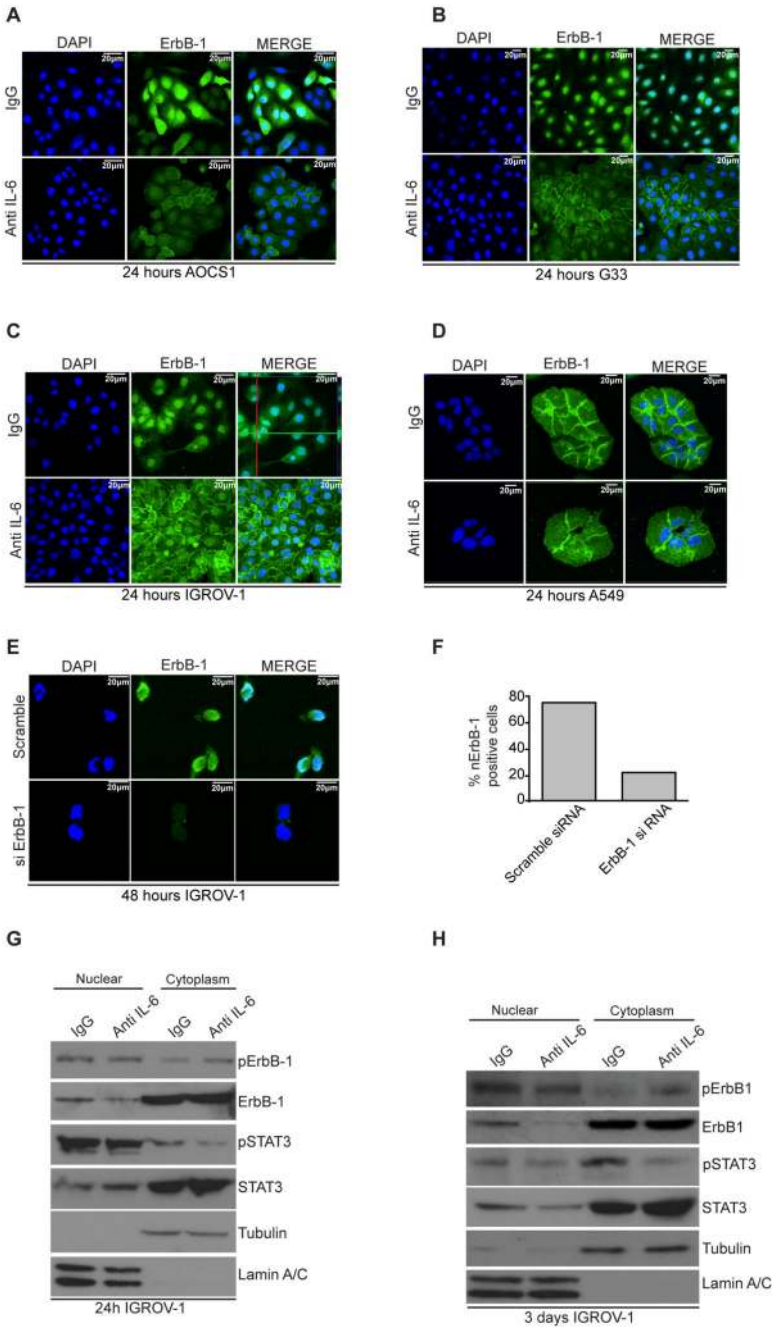

Figure 3. ErbB-1 is located in the nucleus of HGSC cells

A-C. Confocal analysis of HGSC cell lines (AOCS1, G33) and IGROV-1 cells seeded on coverslips and treated with IgG control (10μg/ml) or anti-IL-6 antibody (10μg/ml) for 24 hours. Top panel shows the nuclear localization of ErbB-1 when cells are treated with an IgG control (see green and red lines in C highlighting nuclear localization of ErbB-1 after a z-stack image merge). After treatment with an anti-IL-6 antibody, the amount of ErbB-1 fluorescence in the nucleus is reduced and appears more concentrated at the plasma membrane. **D.** A549 cells treated with an IgG control (top panel) or anti-IL-6 (bottom

panel). Confocal imaging shows ErbB-1 located at the plasma membrane in both groups. **E.** Confocal analysis of IGROV-1 cells transfected with Scramble siRNA (top panel) or siErbB-1 (bottom panel). **F.** Percentage of nErbB-1 positive cells after transfection with Scramble or ErbB-1 siRNA. Results represented on graph correspond to the average obtained in 4 fields analyzed. **G,H**. IGROV-1 cells were treated with an IgG control or an anti-IL-6 antibody for 24hours and 3 days and subjected to nuclear and cytoplasmic fractionation. Tubulin and Lamin A/C were used for a quality control of the cytoplasmic/ nuclear fractionation. Results shown are typical of 3 independent experiments.

Europe PMC Funders Author Manuscripts

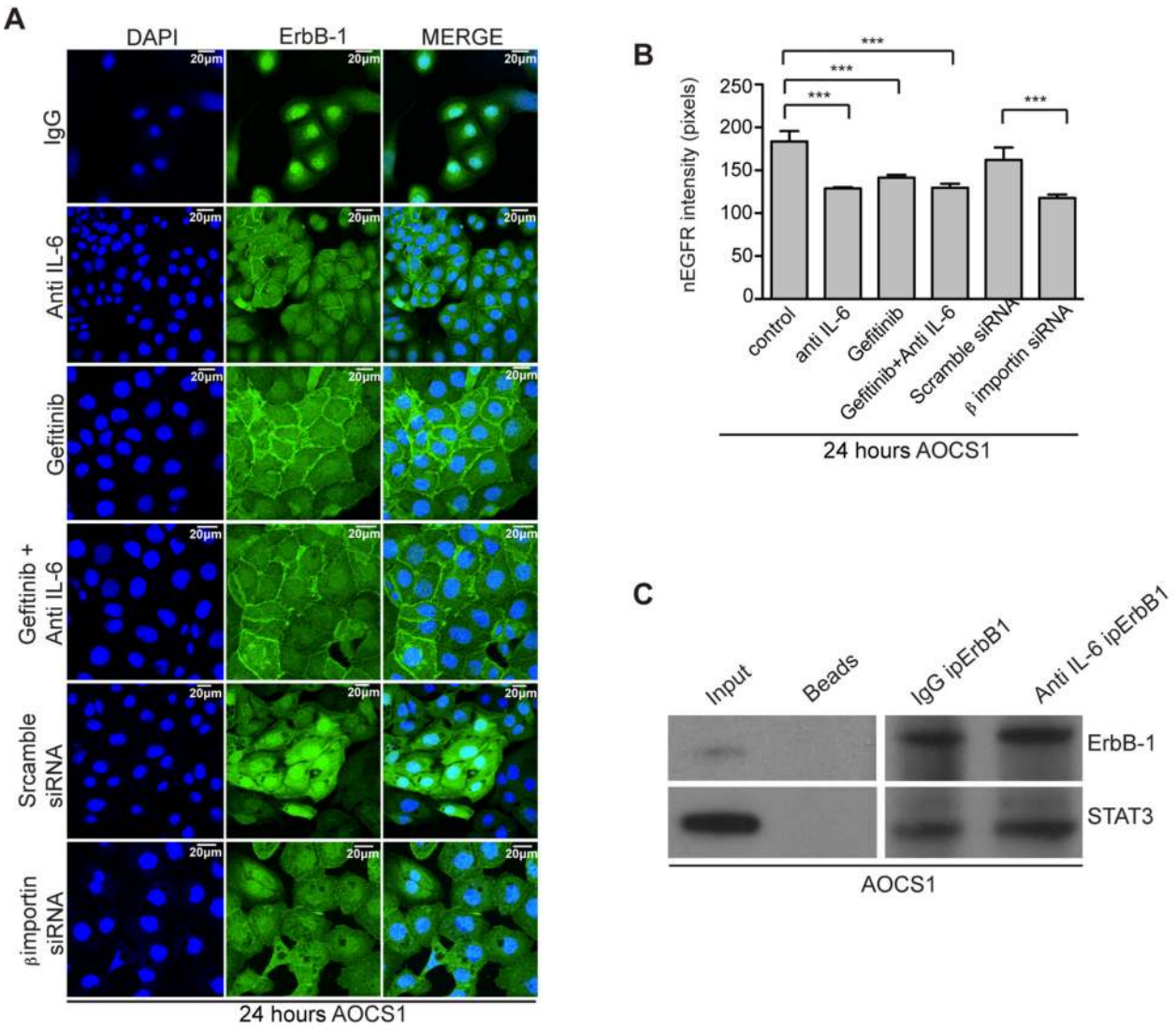

Figure 4. Gefitinib and anti-IL-6 reduces nuclear ErbB-1 in HGSC cells

A. Confocal analysis of AOCS1 cells treated with IgG control, anti-IL-6 antibody, gefitinib, gefitinib+anti-IL-6 antibody, 'scramble' siRNA or β-importin siRNA. After 24 hours, cells were fixed and stained for ErbB-1. Results observed were validated in five independent experiments. **B.** nErbB-1 intensity was quantified using methamorph analysis software. Data correspond to the average of 5HPF analyzed per group. Statistic analysis was performed and is shown as (*) p ≤0.05: (**) p ≤0.01; (***) p ≤0.001. **C.** STAT3 western blot after ErbbB-1 immunoprecipitation in AOCS1 cells.

Europe PMC Funders Author Manuscripts

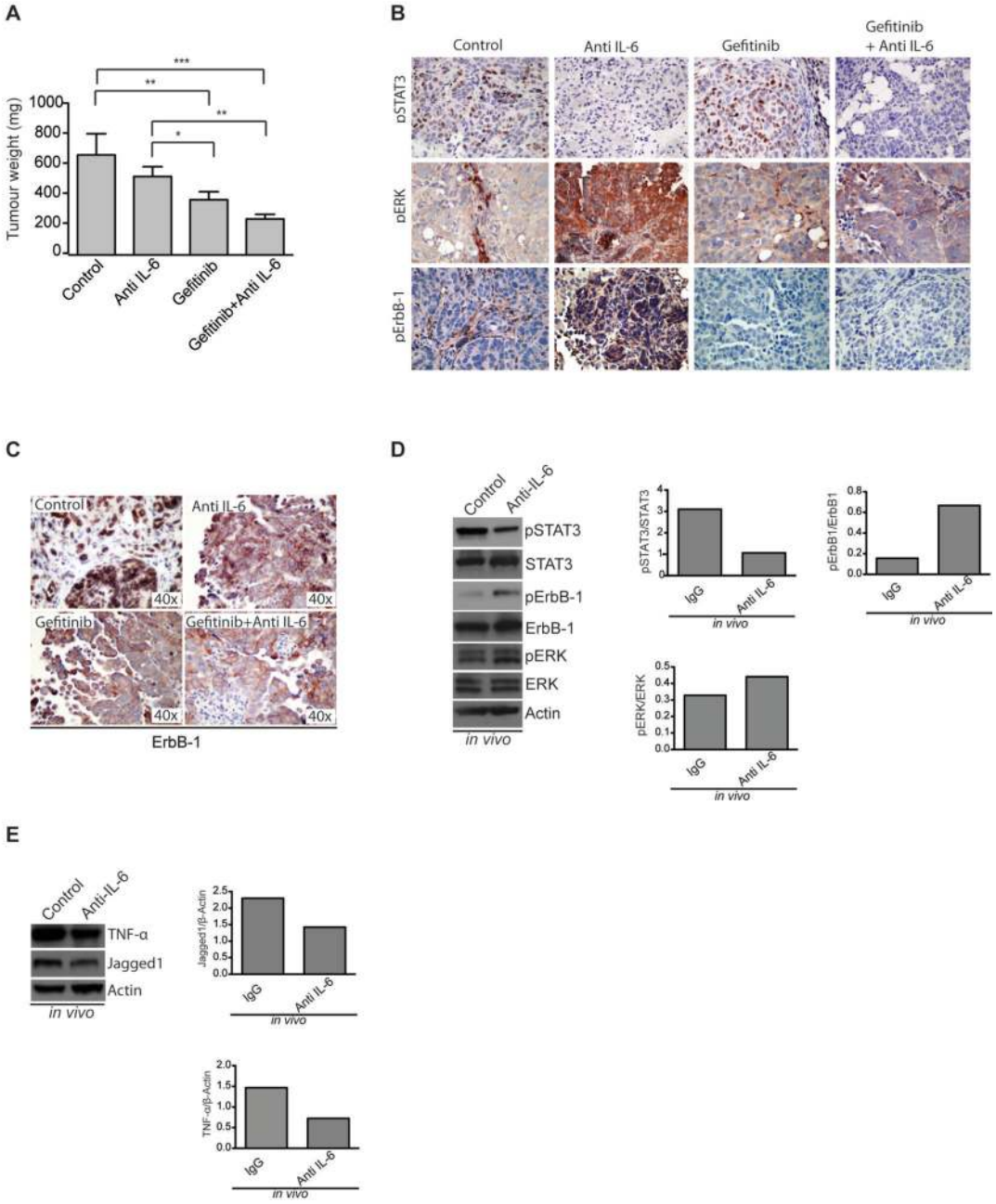

Figure 5. Effects of inhibition of IL-6 and/or ErbB-1 in mouse ovarian cancer xenografts

A. Weight of dissected peritoneal tumors collected from mice injected i.p. with IGROV-1 and treated with either an IgG antibody, an anti-IL-6 antibody, gefitinib or their combination. Data in A are shown as mean ± SEM of 2 independent experiments with a total of 8 mice per experimental group in each experiment Statistic analysis was performed and is shown as (*) p ≤0.05: (**) p ≤0.01; (***) p ≤0.001. **B.** pSTAT3, pERK and pErbB-1 staining on mouse tumor sections from the above experiment. **C.** ErbB-1 staining on mouse tumor sections. **D.** Western blot analysis and quantification of pSTAT3, pErbB-1 and pERK

in protein extracts from mouse xenografts treated with an anti-IL-6 antibody. **E.** Western blot analysis and quantification of TNFα and Jagged1 in protein extracts from mouse xenografts treated with an anti-IL-6 antibody. Quantification was done using ImageJ software and is always relative to the total protein. Results represented on graphs correspond to fold increase.

Europe PMC Funders Author Manuscripts

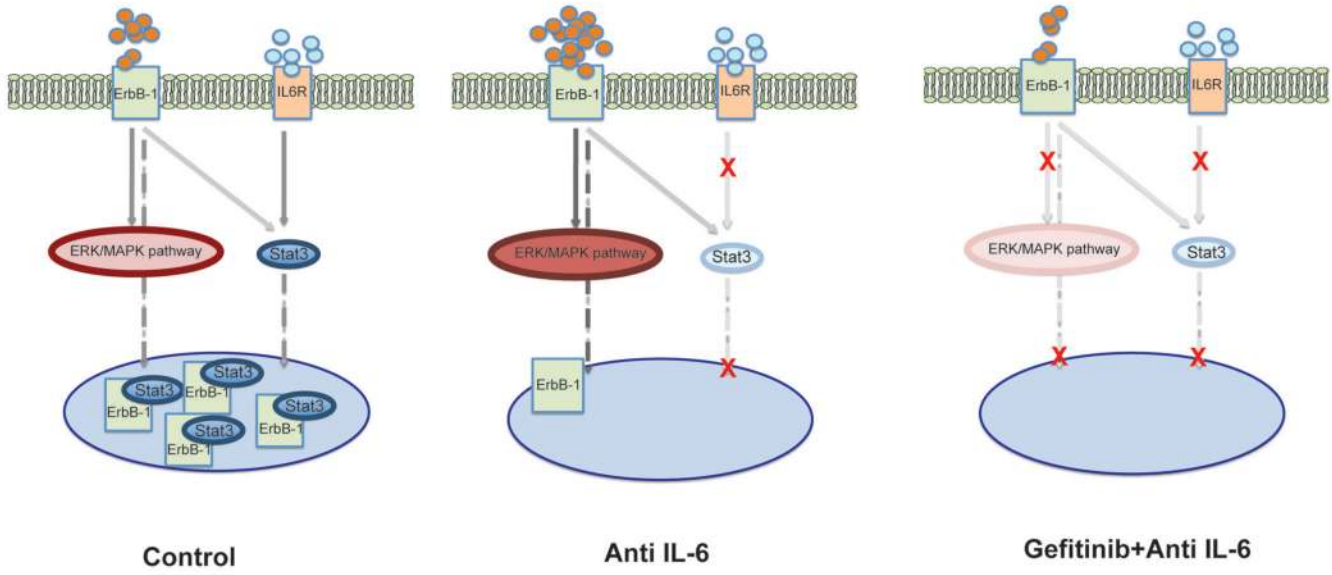

Figure 6. Model for mechanism of action of IL-6 and ErbB-1 signaling inhibition

In control conditions EGFR and IL-6 signaling pathways interact. STAT3 translocates to the nucleus where it interacts with ErbB-1. When IL-6 signaling is inhibited, there is a reduction in available STAT3 in the nucleus. Cells compensate for IL-6 inhibition by activating EGFR family members. nErbB-1 levels are decreased because there is less STAT3. As a result ErbB-1 expression becomes more prominent at the plasma membrane and this is sustained when inhibition of IL-6 is combined with ErbB-1 signaling inhibitors.